Available online at www.sciencedirect.com
SCIENCE DIRECT
Cement and Concrete Research 36 (2006) 671 – 677
Cement and Concrete Research

Effect of temperature on hydration kinetics and polymerization of tricalcium silicate in stirred suspensions of CaO-saturated solutions

Steven A. Grant [a,*], Ginger E. Boitnott [a], Charles J. Korhonen [a], Ronald S. Sletten [b]

[a] U.S. Army Engineer Research and Development Center, Cold Regions Research and Engineering Laboratory, 72 Lyme Road, Hanover, NH 03755-1290, USA
[b] Quaternary Research Center, University of Washington, Seattle, USA

Received 5 October 2005; accepted 5 October 2005

Abstract

Tricalcium silicate was hydrated at 274, 278, 283, 298, and 313 K in stirred suspensions of saturated CaO solutions under a nitrogen-gas atmosphere until the end of deceleratory period. The suspension conductivities and energy flows were measured continuously. The individual reaction rates for tricalcium silicate dissolution, calcium silicate hydrate precipitation, and calcium hydroxide precipitation were calculated from these measurements. The results suggest that the proportion of tricalcium silicate dissolved was determined by the rate of tricalcium silicate dissolution and the time to very rapid calcium hydroxide precipitation. The time to very rapid calcium hydroxide precipitation was more sensitive to changes in temperature than was the rate of tricalcium silicate dissolution, so that the proportion of tricalcium silicate hydration dissolved by the deceleratory period increased with decreasing temperature. The average chain length of the calcium silicate hydrate ascertained by magic-angle spinning nuclear magnetic resonance spectroscopy increased with increasing temperature.
© 2005 Elsevier Ltd. All rights reserved.

Keywords: Calorimetry; Hydration; Kinetics; Temperature; Ca_3SiO_5

1. Introduction

The precipitation of calcium silicate hydrates during portland cement hydration has many of the characteristics of a polymerization reaction—the resulting gel is thermodynamically stable and, while not amenable to X-ray diffraction analysis, is formed by the repetitive addition of segments to the solid structure from solution. Slight changes in the chemical or physical environments in which these reactions occur can have pronounced effects on the hydration rate and the ultimate strength of the portland cement paste. Although antifreeze admixtures have been developed from trial and error, the physical chemistry that dictates the interplay between low temperatures and admixture concentrations with hydration reaction kinetics and the final calcium silicate hydrate structure has not been studied systematically. Specifically, although it is generally known that freezing-point depressing and accelerator admixtures allow rapid curing at low temperatures, there is no sufficient information on the fundamental cement-hydration chemistry to guide the development of admixture blends that will allow for the development of rapid-curing antifreeze admixture blends that will not be susceptible to producing unacceptably weak concrete. To gain additional insight for the development of custom antifreeze admixture blends, we measured continuously the changes of energy flow and solution conductivities of tricalcium silicate in CaO-saturated solutions at 274, 278, 283, 298, and 313 K. The degree of polymerization of the resulting pastes was determined by ^{29}Si magic-angle spinning nuclear magnetic resonance spectroscopy (^{29}Si MAS NMR).

2. Materials and methods

2.1. Hydration experiments

A special calorimetric cell (Figs. 1 and 2) was fabricated to measure continuously energy flow and electrical conductivities in stirred suspensions of Ca_3SiO_5(s) and CaO-saturated aqueous solutions. Since the enthalpies of tricalcium silicate dissolution and calcium silicate hydrate precipitation were greater than that of calcium hydroxide precipitation, the overall energy flow presented the progress of the former two reactions. The molality of

* Corresponding author.
E-mail address: steven.a.grant@usace.army.mil (S.A. Grant).

0008-8846/$ - see front matter © 2005 Elsevier Ltd. All rights reserved.
doi:10.1016/j.cemconres.2005.10.001

Ca^{2+}(aq) was calculated from the solution conductivity. Triclinic tricalcium silicate with a particle diameter no larger than 45 μm and a Blaine fineness of approximately 3000 $cm^2\ g^{-1}$ provided by the Construction Technology Laboratories, Skokie, Illinois, was used in all experiments. The calorimetric cell and experimental details were similar to those described by [1]. Approximately 5 mL CaO saturated solution that was prepared at the experimental temperature under a N_2-gas saturated atmosphere was placed in the calorimetric cell. The calorimetric cell was inserted into a Setaram BT.215 Calvet microcalorimeter housed in a cold room, the temperature of which was set 5 K lower than the experimental temperature. The precision electric heater in the calorimeter maintained the test temperature to within 10 mK of the desired experimental temperature. The solution was stirred by a propeller rotating at 640 rpm. Once thermal equilibrium had been achieved, approximately 0.5 g of tricalcium silicate was dropped into aqueous phase in the calorimetric cell. Energy flow and suspension electrical conductivity were measured every 10 s. The former by the microcalorimeter, the latter by a YSI 3200 Conductivity Instrument measuring AC conductivity at a frequency of 1010 Hz. Hydration was stopped at the end of the deceleratory period at the beginning of the continuing slow reaction period [6]. At the end of the calorimetric experiment, pastes were removed from the calorimetric cell and washed with propanol to halt hydration. The pastes were then dried and subjected to ^{29}Si MAS NMR to determine the intensities (relative to tetramethyl silane) of the Q_0, Q_1, and Q_2 silicon polymerization states in the sample. The polymerization states correspond to the number of Si–O–X bonds maintained by individual silicon atoms and are a direct measure of the nature and development of the calcium silicate hydrate structure in the dried paste.

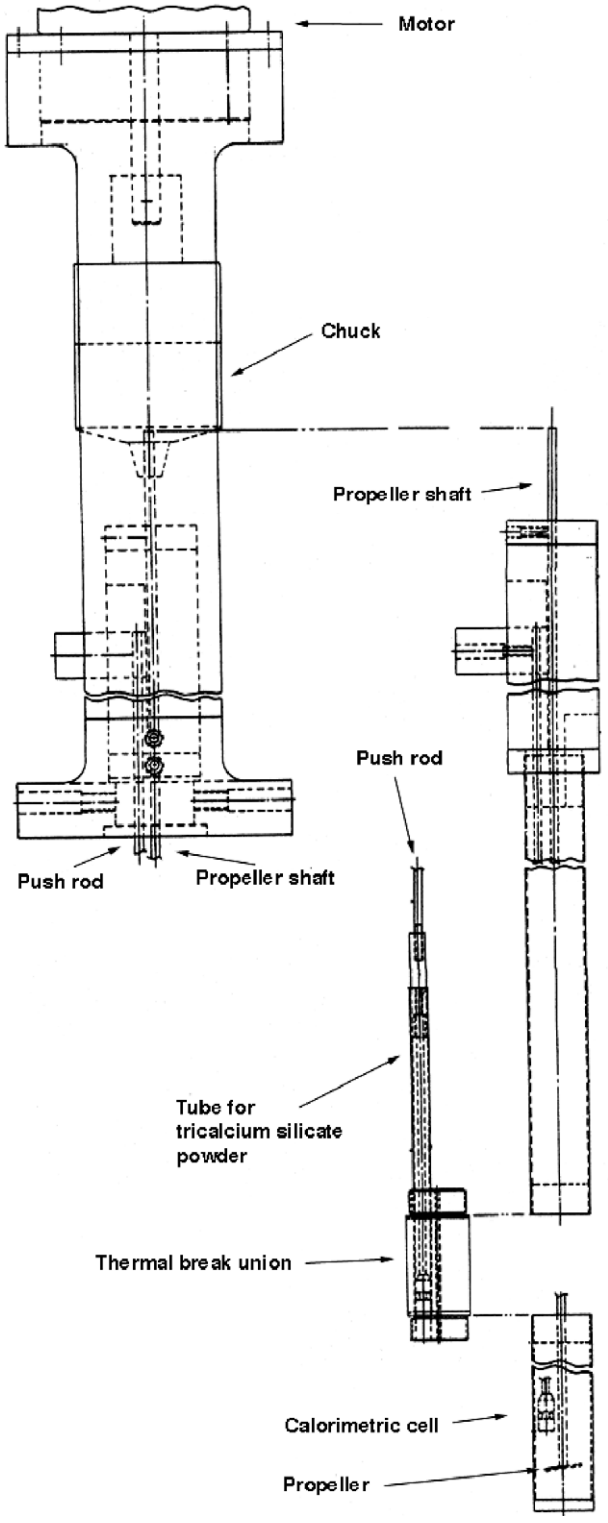

Fig. 1. Assembly drawing of calorimetric cell apparatus.

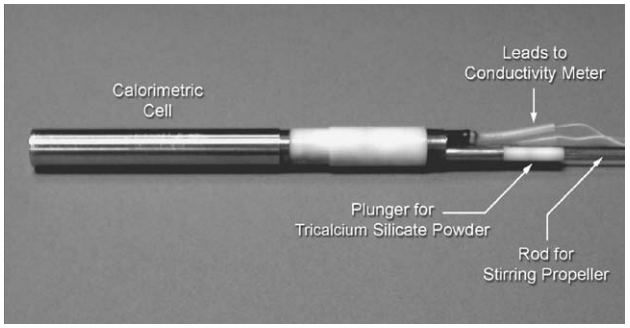

Fig. 2. Photograph of the calorimetric cell showing the shafts for the stirrer and plunger and the leads to the conductivity meter.

2.2. Calculation of individual reaction rates

The reaction rates attending the hydration of tricalcium silicate were elucidated from the measured energy flow and solution conductivity at temperatures from 274 to 313 K. Here we present the:

(1) assumed reaction stoichiometry,
(2) calculated enthalpies of reaction at experimental temperatures, and
(3) correlation of solution conductivity to Ca^{2+} (aq) molality.

2.3. The assumed reaction stoichiometry

The principal reactions in tricalcium silicate hydration are the dissolution of tricalcium silicate,

$$Ca_3SiO_5(s) + 3H_2O(l) = 3Ca^{2+}(aq) + 4OH^-(aq) + H_2SiO_4^{2-}(aq) \qquad \text{(Reaction A)}$$

Table 1
Estimated parameters for general linear model linear regression fit to selected hydrated and unhydrated calcium silicates

		CaO	SiO_2	H_2O	R^2
$-\Delta H$	kJ mol^{-1}	−685.93	−939.66	−293.86	1.00
$-\Delta G$	kJ mol^{-1}	−656.82	−882.49	−234.05	1.00
ΔS	J K^{-1} mol^{-1}	49.38	29.02	33.65	1.00
a	J K^{-1} mol^{-1}	57.83	37.07	11.18	0.98
b	J K^{-1} mol^{-1}	−.015930	0.040723	0.074408	0.86
c	J K^{-1} mol^{-1}	−120421.63	−14464.42	−91163.70	0.94

the precipitation of calcium silicate hydrate,

$$x\mathrm{Ca}^2 + (\mathrm{aq}) + y\mathrm{H_2SiO_4^{2-}}(\mathrm{aq}) + (z-x)\mathrm{H_2O(l)} + 2(x-y)\mathrm{OH^-(aq)} = (\mathrm{CaO})_x(\mathrm{SiO_2})_y(\mathrm{H_2O})_z(\mathrm{s}) \quad \text{(Reaction B)}$$

and the precipitation of calcium hydroxide

$$\mathrm{Ca^{2+}(aq)} + 2\mathrm{OH^-(aq)} = \mathrm{Ca(OH)_2(s)} \quad \text{(Reaction C)}$$

[5]. In CaO-saturated media, calcium silicate hydrate (II) is the dominant silicate participated from the dissolution of tricalcium silicate, for which $x=9$, $y=5$, and $z=11$ [7] and was assumed to be the sole form precipitated in our experiments. While it is doubtful that these stoichiometries are constant during the hydration process, it was assumed that the deviations are not large.

2.4. Calculation of enthalpies of reaction

The standard enthalpy of reaction at 298.15 K ($\Delta_r H°$) was calculated by

$$\Delta_r H° = \sum_{i=products} v_i \Delta_f H_i° - \sum_{i=reactants} v_i \Delta_f H_i° \quad (1)$$

where v_i was the stoichiometric number for substance i and $\Delta_f H_i°$ was its standard enthalpy of formation [8].

$\Delta_r H°$ at another temperature was calculated by

$$\Delta_r H_{T_f}° = \Delta_r H_{T_r}° + \int_{T_r}^{T_f} \Delta_r C_p° dT \quad (2)$$

where $\Delta_r C_p°$ is the change in the heat capacities of the system components due to the reaction, T is temperature, T_r is reference temperature, T_f is observational temperature (all K) [8].

The Gibbs energies of formation, the enthalpies of formation, the entropies, and parameters of the Maier-Kelly equation for calcium silicate hydrates as functions of composition were estimated by general-linear-model regression of the thermodynamic properties of 13 calcium silicates presented in [10] to the equation

$$y = \beta_{y,\mathrm{CaO}} v_{\mathrm{CaO}} + \beta_{y,\mathrm{SiO_2}} v_{\mathrm{Si_2O}} + \beta_{y,\mathrm{H_2O}} v_{\mathrm{H_2O}} \quad (3)$$

where y was the thermodynamic property fitted; v_{CaO}, $v_{\mathrm{SiO_2}}$, and $v_{\mathrm{H_2O}}$ were the numbers of each component in the solid, and $\beta_{y,\mathrm{CaO}}$, $\beta_{y,\mathrm{SiO_2}}$, and $\beta_{y,\mathrm{H_2O}}$ were the corresponding fitted parameters.

The parameter estimates and the coefficient of determination R^2 are presented in Table 1, in which the quantities a, b, and c are parameters in the Maier-Kelly equation:

$$C_p = a + bT + c/T^2 \quad (4)$$

where C_p is constant-pressure heat capacity (kJ K^{-1} mol^{-1}). These estimated values for the thermodynamic properties of the calcium silicate hydrates and standard values found in the published literature are presented in Table 2.

2.5. Calculation of Ca solution concentrations

The solution concentrations of Ca^{2+} (aq) in the CaO-saturated solutions were assumed to be equal to the solubilities of $Ca(OH)_2$ as reported from a critical review of all published data [12]. From this concentration and the measured conductivity before hydration began, the linear relationship between conductivity and Ca^{2+} (aq) was established for each hydration experiment.

2.6. Calculation of reaction rates

Reaction rates during each period were calculated by relating the measured energy flux and solution conductivities to changes in reaction enthalpies and solution Ca^{2+} (aq) concentration. The total energy flow per kg of solvent, q (W

Table 2
Thermodynamic values pertinent to tricalcium silicate hydration

Compound	M (kJ mol^{-1})	$\Delta_f G°$ (298.15 K) (kJ mol^{-1})	$\Delta_f H°$ (298.15 K) (kJ mol^{-1})	$S°$ (298.15 K) (J K^{-1} mol^{-1})	C_p (298.15 K) (J K^{-1} mol^{-1})	Ref.
H_2O (l)	0.0180148	−237.141	−285.830	69.95	75.295	[9]
Ca^{2+} (aq)	0.0400780	−553.076	−543.0	−56.2	0.8	[9]
OH^{1-} (aq)	0.0170069	−157.381	−230.015	−10.90	−149.	[9]
H_4SiO_4 (aq)	0.0961136	−1309.254	−1460.7	179.	215.	[10]
$H_3SiO_4^-$ (aq)	0.0951057	−1253.486	−1424.9	113.	−72.4	[10]
$H_2SiO_4^{2-}$ (aq)	0.0940978	−1186.916	−1395.5	−13.	−280.	[10]
$Ca(OH)_2$ (cr)	0.0740918	−898.421	−986.59	76.1	84.5	[11]
Ca_3SiO_5 (s)	0.2283150	−2786.190	−2929.202	168.599	171.878	[10]
$(CaO)(SiO_2)(H_2O)_2$ (s)	0.1521906	−2007.41	−2213.31	145.70	165.45	[10]
$(CaO)_2(SiO_2)(H_2O)_2$ (s)	0.2082676	−2664.23	−2899.24	195.08	217.18	[10]
$(CaO)_5(SiO_2)_5(H_2O)_6$ (s)	0.6888939	−9100.85	−9891.11	593.90	697.91	[10]
$(CaO)_9(SiO_2)_5(H_2O)_{11}$ (s)	1.0032758	−12898.38	−14104.13	959.67	1066.51	[10]

Table 3
Standard enthalpies for Reaction (A), Reaction (B), and Reaction (C) at the temperatures at which experiments were conducted

T (K)	$\Delta_r H°$ (kJ mol^{-1})								
	Reaction (A)	Reaction (B)							Reaction (C)
		Values of x, y, and z							
		1,1,2	2,1,2	5,5,6	6,5,7	7,5,9	8,5,10	9,5,11	
313.15	−176.9	16.6	54.2	117.5	145.2	166.7	195.7	224.7	22.2
298.15	−157.9	11.0	42.3	87.2	110.5	125.7	148.9	172.2	16.4
283.15	−138.8	5.5	30.4	56.9	75.7	84.6	102.1	119.6	10.7
278.15	−132.4	3.6	26.4	46.8	64.1	70.9	86.5	102.1	8.8
274.15	−127.4	2.2	23.2	38.8	54.9	60.0	74.0	88.1	7.3

kg^{-1}), was assumed to be equal to the weighted sums of the three reaction enthalpies

$$q = \frac{d\xi_A}{dt}\Delta_r H_A^\circ + \frac{d\xi_B}{dt}\Delta_r H_B^\circ + \frac{d\xi_C}{dt}\Delta_r H_C^\circ \quad (5)$$

where ξ_i was the extent of reaction i (mol kg^{-1}), t is time (s) and $\Delta_r H_i^\circ$ is the standard enthalpy for reaction i (J mol^{-1}).[1] (The calculation of these enthalpies as functions of temperatures is discussed in Section 2.2.) These standard reaction enthalpies are presented in Table 3. The reaction rates were related to the changes in Ca^{2+} (aq) molality via

$$\frac{dm_{Ca^{2+}(aq)}}{dt} = 3\frac{d\xi_A}{dt} - 9\frac{d\xi_B}{dt} - \frac{d\xi_C}{dt}. \quad (6)$$

Silicate solution molalities in tricalcium silicate pastes have been found to be trivial in comparison to those of calcium [13]. For the purposes of calculating reaction rates, one could assume that the change in the amount of silicate in solution was nil:

$$\frac{dm_{H_2SiO_4^{2-}(aq)}}{dt} \approx 0. \quad (7)$$

By inspection of reactions (A), (B), and (C), one could write directly

$$\frac{dm_{H_2SiO_4^{2-}(aq)}}{dt} = \frac{d\xi_A}{dt} - 5\frac{d\xi_B}{dt}. \quad (8)$$

So we assumed that

$$\frac{d\xi_A}{dt} = 5\frac{d\xi_B}{dt}. \quad (9)$$

Eqs. (5), (6) and (9) were three equations with three unknowns that could be solved directly by linear algebra.

3. Results

3.1. General observations of the sequence of reaction maxima

Fig. 3 presents the measured Ca^{2+} (aq) molality and energy flow for an experiment run at 298 K. The energy flow and

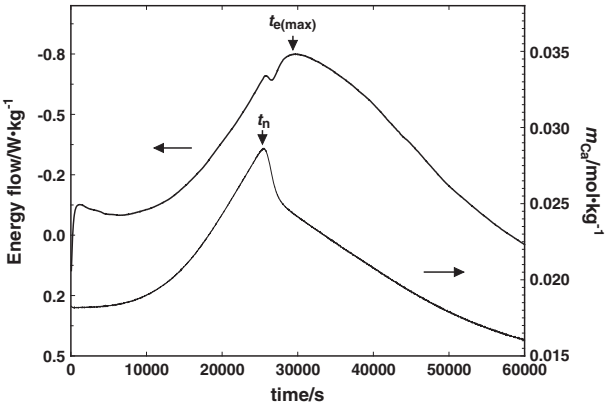

Fig. 3. Energy flow (upper curve) and solution Ca^{2+} (aq) molality (lower curve) measured simultaneously during hydration experiment conducted at 298 K with time to very rapid $Ca(OH)_2$ precipitation (t_n) and maximum energy flow ($t_{e(max)}$) indicated.

Ca^{2+} (aq) molality curves were both broad, asymmetric peaks. The peak in Ca^{2+} (aq) molality had a single maximum (denoted by t_n), whereas the energy flow peak had two. The first local maximum on the energy flow peak (which has not been observed in calorimetric studies of tricalcium silicate pastes [2]) coincided with t_n and was followed by the second peak at which the energy flow was greatest, designated $t_{e(max)}$ (Fig. 4).

There is an on-going question as to whether experiments conducted on tricalcium silicate suspensions are comparable to experiments on tricalcium silicate and cement pastes. For example, a careful study of tricalcium silicate hydration in water at water-to-solid (w/s) weight ratios of 0.7 to 20 found a pronounced effect of w/s ratios [13]. For the suspensions studied, calcium dissolved in solution decreased, silicate in solution increased, extent of the hydration reaction increased, and rate of reaction increased with increasing w/s ratio. In a similar study, Barret and Bertrandie argued that the extent of the hydration reaction and length of the induction period was determined largely by the amount of calcium released by the dissolution of the tricalcium silicate [14]. The higher the w/s ratio, the more calcium released by tricalcium silicate dissolution and the longer the acceleratory period and more

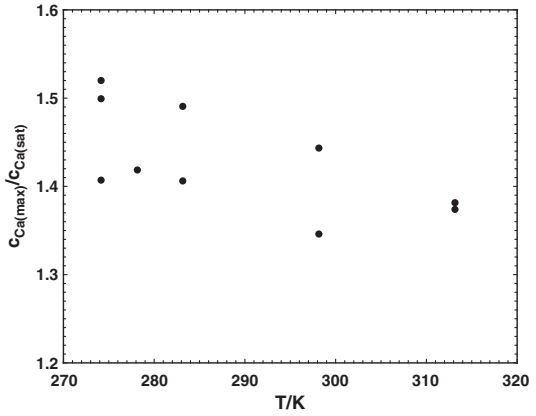

Fig. 4. Apparent degree of Ca^{2+} (aq) supersaturation at time of very rapid $Ca(OH)_2$ precipitation as affected by experimental temperature.

[1] Extent of reaction is defined by IUPAC as: "Extensive quantity describing the progress of a chemical reaction equal to the number of chemical transformations, as indicated by the reaction equation on a molecular scale, divided by the Avogadro constant (it is essentially the amount of chemical transformations)" [19].

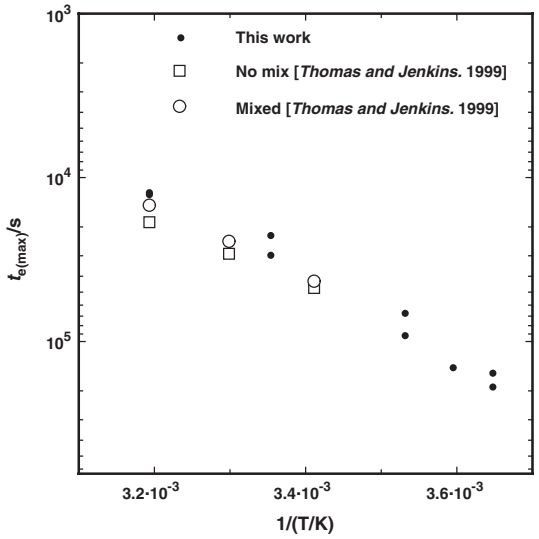

Fig. 5. Values of $t_{e(max)}$ determined in this study and those reported by [2].

of the C3S is converted to calcium silicate hydrate. Nonat et al. argued that these effects could be limited by hydrating tricalcium silicate in solutions of deaerated water saturated with respect to freshly prepared calcite, which limits the amount of calcium released by dissolution of tricalcium silicate [15]. Comparison of our results with a similar study on pastes supports the assertion by Nonat et al. Fig. 5 presents an Arrhenius plot of the $t_{e(max)}$ values measured in this study and those on mixed and unmixed tricalcium silicate pastes reported by [2]. The value $t_{e(max)}$ appeared to be achieved at earlier times in the suspensions than in pastes, presumably because diffusional effects were lessened by the continuous mixing of the suspension. Other than this shift, the data appear to be comparable. Calculation of apparent activation energies yielded the following values for unmixed pastes: 35.26±0.16 kJ mol^{-1} (R^2=1.00), mixed pastes 40.67±0.41 kJ mol^{-1} (R^2=1.00) [2], and this study 49.15±2.71 kJ mol^{-1} (R^2=0.98). Interestingly, the apparent activation energy calculated from only those data comparable to those of the study of [2] 298 and 313 K was 37.62±7.22 kJ mol^{-1} (R^2=0.93). This result suggests that the results on this study regarding the effect of temperature are comparable to what would be observed in pastes (Fig. 4).

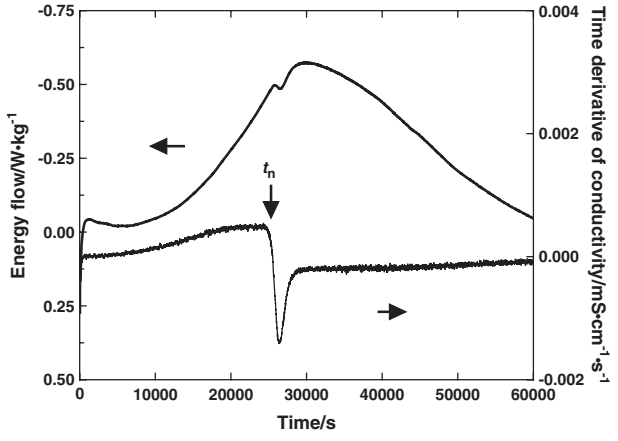

Fig. 6. Energy flow (upper curve) and time derivative of solution conductivity (lower curve) for hydration experiment run at 298 K, with t_n, time of very rapid $Ca(OH)_2$ precipitation.

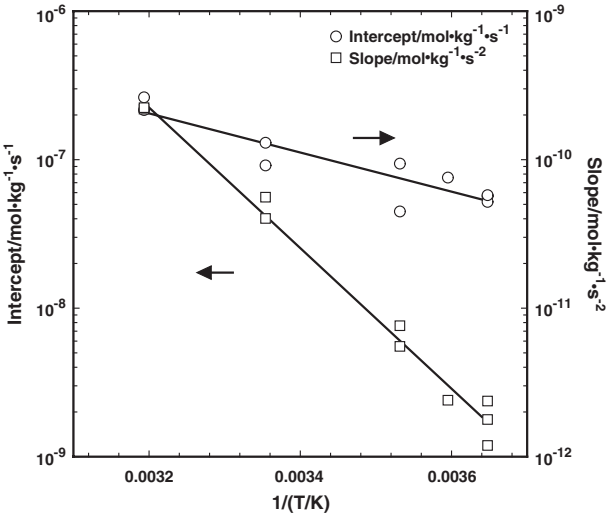

Fig. 7. Arrhenius plot of the slope (upper curve) and intercept (lower curve) of the linear regression dCa^{2+} (aq)/dt before t_n against time.

We found that replacing the conductivity data with its time derivative, as is done here in Fig. 6, gave a better sense of the sequence of reactions in solution. The time derivative of conductivity revealed clearly the abrupt change in Ca^{2+} (aq) concentration, marked in Fig. 6 by t_n, time to very rapid $Ca(OH)_2$ precipitation. The time derivative of conductivity is almost linear between the onset of hydration and t_n. Linear regression was performed on the values of dCa^{2+} (aq)/dt (a simple transformation that allowed comparison of the values for the for the various temperatures) before t_n. Fig. 7 presents an Arrhenius plot of the slope and intercept of these linear regression. The corresponding apparent activation energies were obtained for the intercept 25.22±3.96 kJ mol^{-1} (R^2=0.84) and the slope 90.62±3.64 (R^2=0.99).

As shown in Fig. 8 we observed that t_n consistently occurred before $t_{e(max)}$ at all experimental temperatures.

These results indicated that the maximum rates of tricalcium silicate dissolution and calcium silicate hydrate precipitation

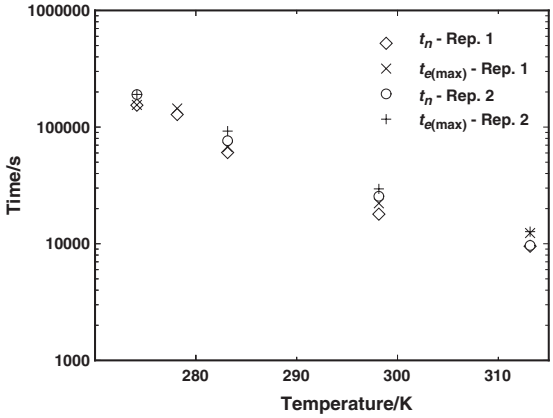

Fig. 8. Correspondence of time of the maximum energy flow and time to very rapid $Ca(OH)_2$ precipitation.

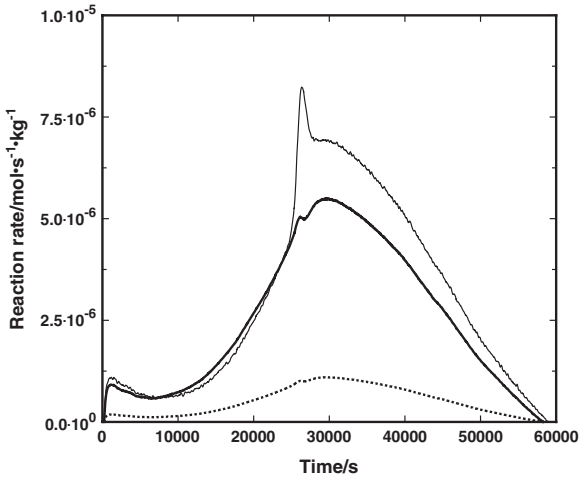

Fig. 9. Rates of reactions (A) (bold line), (B) (dashed line), and (C) (thin line) for hydration experiment run at 298 K.

occurred just after the onset of very rapid $Ca(OH)_2$ precipitation. It has been argued that the precipitation of calcium hydroxide in stirred suspensions was extraneous to the dissolution of tricalcium silicate and precipitation of calcium silicate hydrate [4,14]. The close correlation between t_n and $t_{e(max)}$ challenges that argument.

3.2. Individual reaction rates

Fig. 9 presents the calculated rates of reactions (A), (B) and (C) for a hydration experiment conducted at 298 K. By this calculation, one can see that t_n did indeed correspond to the very rapid increase in the rate of calcium hydroxide precipitation and $t_{e(max)}$ corresponded to the maximum rates of tricalcium silicate dissolution and calcium silicate hydrate precipitation. Fig. 10 presented the initial rate of reaction A and the time to very rapid $Ca(OH)_2$ precipitation as functions of reciprocal temperature. A fit of these data to the Arrhenius equation yielded apparent activation energies of 39.25 ± 6.43 kJ mol^{-1} ($R^2 = 0.84$) for $d\xi_A/dt$ and 53.17 ± 2.86 kJ mol^{-1} ($R^2 = 0.98$) for t_n. One could conclude that the time to very rapid $Ca(OH)_2$ precipitation is more sensitive to temperature than is the rate of tricalcium silicate dissolution. As temperature decreases one would expect that more tricalcium silicate to dissolve before very rapid $Ca(OH)_2$ precipitation occurs, marking the beginning of the end of increasing tricalcium silicate hydration. Fig. 11 presented the fraction of tricalcium silicate dissolved as determined by the total heat flows measured during the experiment. The fraction of tricalcium silicate dissolved increased with decreasing temperature, as would have been expected by the differing temperature sensitivities of tricalcium silicate dissolution and very rapid $Ca(OH)_2$ precipitation. The proportion of tricalcium silicate dissolved through the deceleratory period is likely to play a role in determining the initial and final set as well as the rates of initial hardening and early strength gain [16].

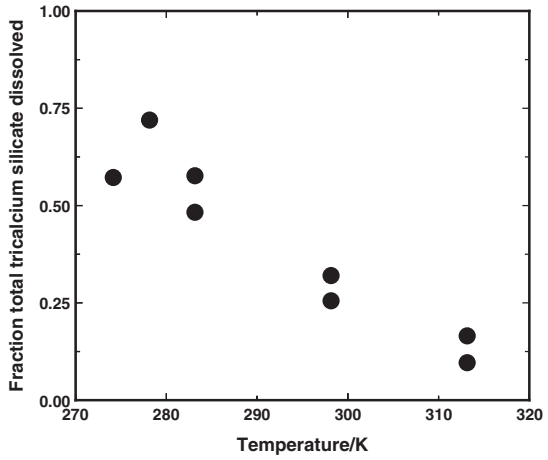

Fig. 11. Calculated fraction of tricalcium silicate dissolved by the end of the deceleratory period at the indicated experimental temperatures.

These results presented a physical basis for the observation that cements cured at low temperatures had greater ultimate strengths than cements cured at room temperature [17]. While the rate of tricalcium silicate dissolution was lowered at lower temperatures, the time to very rapid $Ca(OH)_2$ precipitation was delayed proportionally even more—allowing a greater fraction

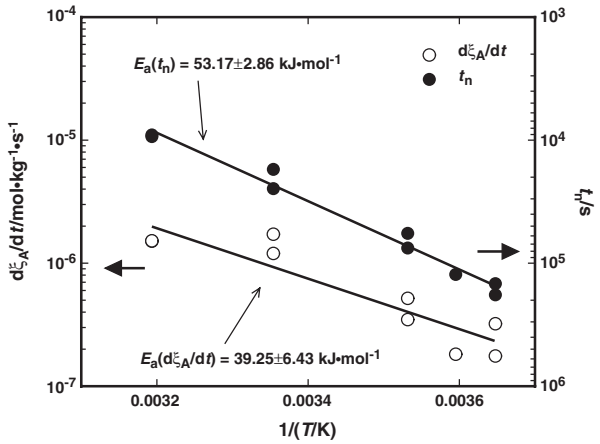

Fig. 10. Arrhenius plot showing a comparison of effect of temperature on initial rate of reaction (A) and time to very rapid $Ca(OH)_2$ precipitation.

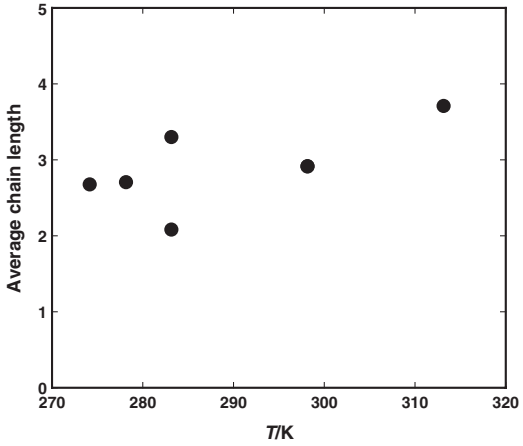

Fig. 12. Estimated average chain lengths of tricalcium silicate pastes hydrated at 274, 278, 283, 298, and 313 K.

of the system tricalcium silicate to dissolve and form calcium silicate hydrate.

3.3. Cross-polarization magic-angle spinning nuclear magnetic resonance spectroscopy analysis

The average chain lengths were to be estimated from the relative intensities of Q_1 and Q_2 determined in ^{29}Si MAS NMR spectra. The average estimated chain lengths are presented in Fig. 12, which indicated that they increased slightly with temperature. Increase in the degree of polymerization with curing temperature has been reported previously [18]. The increase in strength development in tricalcium silicate cured at low temperatures is probably not due to greater degree of polymerization, but rather due to a greater proportion of the tricalcium silicate dissolved by the end of the deceleratory period at lower temperatures.

4. Concluding remarks

We determined the rates of the individual chemical reactions attending the hydration of tricalcium silicate. For all temperatures, we found that time to very rapid $Ca(OH)_2$ precipitation was followed by the maximum rates of tricalcium silicate dissolution and calcium silicate hydrate precipitation. This sequence suggests that the time to very rapid $Ca(OH)_2$ precipitation and the extent of the hydration reaction are related, though the exact mechanism that effects this relation was not elucidated. We also found that the time to very rapid $Ca(OH)_2$ precipitation was more sensitive to changes in temperature than was the rate of tricalcium silicate dissolution. This suggests that the fraction of tricalcium silicate dissolved should increase with increasing temperature. Such a trend was observed from the specific integral energy flow at the experimental temperatures. This suggests a mechanistic explanation for the observation that cements cured at low temperature tend to have greater ultimate strengths than those cured at higher temperatures, albeit at a slow rate of early-age curing. Future research should be directed to developing an understanding of the mechanisms controlling strength development. A subsequent article will present our research into the effects of temperature and concrete admixtures on the kinetics of tricalcium silicate hydration.

Acknowledgements

This work was supported by the U.S. Army Engineer Research and Development Center, work unit 61102/AT24/129/EE005, Physical Chemistry and Kinetics of Portland Cement Hydration.

References

[1] D. Damidot, D.A. Nonat, P. Barret, J. Am. Ceram. Soc. 73 (1990) 3319.
[2] J.J. Thomas, H.M. Jennings, Chem. Mater. 11 (1999) 1907.
[4] S. Gauffinet, L. Nachbaur, A. Nonat, in: A. Negro, L. Montanaro (Eds.), Proceeding for EUROSOLID 4, Politecnico di Torino, Turin, Italy, 1997.
[5] F. Tzschichholz, H.J. Herrmann, H. Zanni, Phys. Rev., E Stat. Phys. Plasmas Fluids Relat. Interdiscip. Topics 53 (1996) 2629.
[6] H.F.W. Taylor, Cement Chemistry, 2nd ed., Thomas Telford, London, 1997, p. 150.
[7] H.F.W. Taylor, Cement Chemistry, 2nd ed., Thomas Telford, London, 1997, p. 130.
[8] K.S. Pitzer, Thermodynamics, 3rd ed., McGraw-Hill, New York, 1995.
[9] J.D. Cox, D.D. Wagman, V.A. Medvedev, CODATA Key Values for Thermodynamics, Hemisphere Publishing Corp., New York, 1989.
[10] V.I. Babushkin, G.M. Matveyev, O.P. Mchedlov-Petrossyan, in: B.N. Frenkel, V.A. Terentyev (Eds.), Thermodynamics of Silicates, Trans, Springer-Verlag, New York, 1985.
[11] I. Barin, Thermochemical Data of Pure Substances, VCH, New York, 1993.
[12] I. Lambert, H.L. Clever (Eds.), Alkaline Earth Hydroxides in Water and Aqueous Solutions, Solubility Data Series, vol. 52, Pergamon Press, Oxford, 1992.
[13] P.W. Brown, E. Franz, G. Frohnsdorff, H.F.W. Taylor, Cem. Concr. Res. 14 (1984) 257.
[14] P. Barret, D. Bertrandie, Solid State Ion. 101–103 (1997) 359.
[15] A. Nonat, J.C. Mutin, X. Lecoq, S.P. Jiang, Solid State Ion. 101–103 (1997) 923.
[16] S. Mindness, J.F. Young, Concrete, Prentice-Hall, Englewood, NJ, 1981, p. 78.
[17] S. Mindness, J.F. Young, Concrete, Prentice-Hall, Englewood, NJ, 1981, p. 305.
[18] J. Hirljac, Z.-Q. We, J.F. Young, Cem. Concr. Res. 13 (1983) 877.
[19] A.D. McNaught, A. Wilkinson, Compendium of Chemical Terminology, 2nd ed., Blackwell, Oxford, 1997.